AD-A133 819 CYCLIC ROTATION OF PRINCIPAL PLANES TO INVESTIGATE 1/1
LIQUEFACTION OF SANDS(U) ARMY ENGINEER WATERWAYS
EXPERIMENT STATION VICKSBURG MS GEOTE..
UNCLASSIFIED R T DONAGHE ET AL. SEP 83 WES/MP/GL-83-24 F/G 8/13 NL

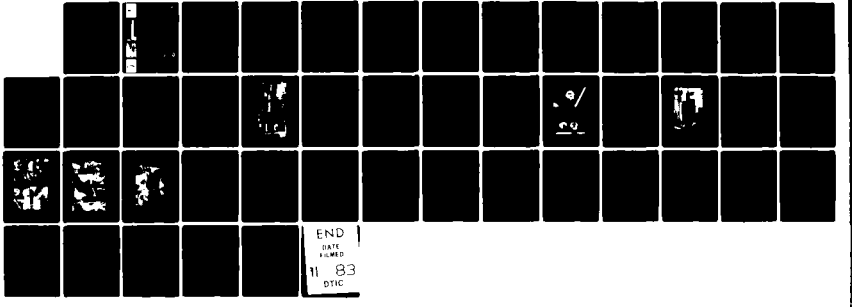

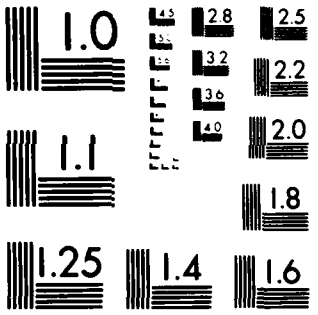

US Army Corps of Engineers

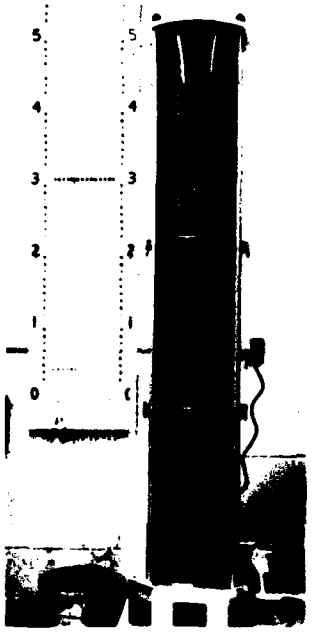

GEOTECHNICAL LABORATORY

MISCELLANEOUS PAPER GL-83-24

CYCLIC ROTATION OF PRINCIPAL PLANES TO INVESTIGATE LIQUEFACTION OF SANDS

by

Robert T. Donaghe, Paul A. Gilbert

Geotechnical Laboratory
U. S. Army Engineer Waterways Experiment Station
P. O. Box 631, Vicksburg, Miss. 39180

September 1983
Final Report

Prepared for Assistant Secretary of the Army (R&D)
Department of the Army
Washington, D. C. 20315

Under Project 4A161101A91D, Task 02
Work Unit 143 Q6

Destroy this report when no longer needed. Do not return it to the originator.

The findings in this report are not to be construed as an official Department of the Army position unless so designated by other authorized documents.

The contents of this report are not to be used for advertising, publication, or promotional purposes. Citation of trade names does not constitute an *official endorsement* or approval of the use of such commercial products.

Unclassified

SECURITY CLASSIFICATION OF THIS PAGE (When Data Entered)

REPORT DOCUMENTATION PAGE		READ INSTRUCTIONS BEFORE COMPLETING FORM
1. REPORT NUMBER Miscellaneous Paper GL-83-24	2. GOVT ACCESSION NO. AD-A133819	3. RECIPIENT'S CATALOG NUMBER
4. TITLE (and Subtitle) CYCLIC ROTATION OF PRINCIPAL PLANES TO INVESTIGATE LIQUEFACTION OF SANDS		5. TYPE OF REPORT & PERIOD COVERED Final report 6. PERFORMING ORG. REPORT NUMBER
7. AUTHOR(s) Robert T. Donaghe Paul A. Gilbert		8. CONTRACT OR GRANT NUMBER(s)
9. PERFORMING ORGANIZATION NAME AND ADDRESS U. S. Army Engineer Waterways Experiment Station Geotechnical Laboratory P. O. Box 631, Vicksburg, Miss. 39180		10. PROGRAM ELEMENT, PROJECT, TASK AREA & WORK UNIT NUMBERS Project 4A161101A91D, Task 02, Work Unit 143 Q6
11. CONTROLLING OFFICE NAME AND ADDRESS Assistant Secretary of the Army (R&D) Department of the Army Washington, D. C. 20315		12. REPORT DATE September 1983 13. NUMBER OF PAGES 41
14. MONITORING AGENCY NAME & ADDRESS(if different from Controlling Office)		15. SECURITY CLASS. (of this report) Unclassified 15a. DECLASSIFICATION/DOWNGRADING SCHEDULE

16. DISTRIBUTION STATEMENT (of this Report)

Approved for public release; distribution unlimited.

17. DISTRIBUTION STATEMENT (of the abstract entered in Block 20, if different from Report)

18. SUPPLEMENTARY NOTES

Available from National Technical Information Service, 5285 Port Royal Road, Springfield, Va. 22161.

19. KEY WORDS (Continue on reverse side if necessary and identify by block number)

Liquefaction
Hollow cylinder
Principal stress rotation
Sand

20. ABSTRACT (Continue on reverse side if necessary and identify by block number)

This report contains a description of a new hollow cylinder soil testing device and results of a preliminary testing program utilizing the device. The objective of the investigation was to design and fabricate a testing device that would apply synchronized cyclic axial and torsional stresses to a hollow cylinder saturated sand specimen in such a manner that there is a continuous and systematic rotation of principal stress axes. Another was to conduct a preliminary testing program and to investigate the effects of (Continued)

DD FORM 1 JAN 73 1473 EDITION OF 1 NOV 65 IS OBSOLETE

Unclassified

SECURITY CLASSIFICATION OF THIS PAGE (When Data Entered)

20. ABSTRACT (Continued).

cyclic rotation of principal stresses in saturated sand specimens in terms of the susceptibility of these materials to earthquake induced liquefaction. Cyclic triaxial tests do not provide for any continuous principal stress rotation during shear (the maximum principal stress does alternate between horizontal and vertical planes) and other tests such as the cyclic simple shear test provide only limited rotation ($\pm$4 deg). Since earthquakes may produce random rotation of principal stresses in situ, a laboratory test having the capability to study principal stress rotation is needed. In the test developed herein, principal stress axes rotate through 360 deg each loading cycle and every plane within the specimen is loaded with the maximum shear stress each cycle. This means that the weakest plane in anisotropic materials will be loaded as intensely as any plane; therefore, the strength and stability of the material will naturally be affected and the consequent effect of anisotropy will be included in the cyclic principal stress rotation test. In the past this effect has only been estimated and the stability of materials determined in the cyclic triaxial test reduced by an empirical factor as a result. In general, cyclic triaxial loading applies maximum shear stress to only one pair of orthogonal planes in a specimen and they are unlikely to be the weakest. Therefore, in anisotropic materials the cyclic triaxial test, and generally any test which does not effect principal stress rotation, will indicate too high a strength. The objectives of the investigation were achieved by designing and building an electropneumatic loading system for an existing hollow cylinder test chamber that satisfied the complex loading requirements and by performing five consolidated-undrained hollow cylinder cyclic principal stress rotation tests on saturated specimens of Monterey No. 0 sand compacted to 50 percent relative density and consolidated under a confining pressure of 1.0 kg/cm^2. Results of the tests indicate that principal stress rotation produced lower laboratory cyclic strength than either cyclic triaxial or cyclic simple shear tests. Additional testing on hollow cylinder cyclic triaxial and simple shear tests are needed over a broader range of variables to verify this finding.

PREFACE

This investigation was conducted by the Geotechnical Laboratory (GL), U. S. Army Engineer Waterways Experiment Station (WES), during the period December 1980 to September 1983 under the Authority of an In-House Laboratory Independent Research Program as Project 4A161101A91D, Task 02, Work Unit 143 Q6, sponsored by the Assistant Secretary of the Army (R&D).

The study was conducted by Messrs. Robert T. Donaghe and Paul A. Gilbert, Soils Research Facility, Soils Research Center, Soil Mechanics Division (SMD), GL, under the supervision of Mr. G. P. Hale, Chief, Soils Research Center, and Mr. C. L. McAnear, Chief, SMD, GL. The work was under the general direction of Dr. William F. Marcuson III, Chief, GL, and Dr. Paul F. Hadala, Assistant Chief, GL. Mr. Donaghe and Mr. Gilbert were the authors of the report.

Commanders and Directors of WES during the conduct of the study were COL Nelson P. Conover, CE, and COL Tilford C. Creel, CE. The Technical Director was Mr. Fred R. Brown.

CONTENTS

CONVERSION FACTORS, U. S. CUSTOMARY TO METRIC (SI) UNITS OF MEASUREMENT

U. S. customary units of measurement used in this report can be converted to metric (SI) units as follows:

Multiply	By	To Obtain
inches	2.54	centimetres
pounds (mass)	0.45359237	kilograms
pounds (mass) per cubic foot	16.0185	kilograms per cubic metre
pounds (force) per square inch	6894.757	pascals

CYCLIC ROTATION OF PRINCIPAL PLANES TO INVESTIGATE LIQUEFACTION OF SANDS

PART I: INTRODUCTION

1. Liquefaction failures occur most frequently in deposits of loose saturated sands under the action of earthquake excitation. The ground motion is three-dimensional and random with time. All components of a general stress tensor at a point within the deposit vary with time and principal stress trajectories at the point rotate in a complex manner which is not well understood.

2. The cyclic triaxial test is the most common laboratory test used to evaluate earthquake liquefaction susceptibility. Soil strengths determined from the test are compared to shear stresses with one- and two-dimensional stress wave propagation computer codes to determine if liquefaction will occur as a result of the earthquake. Specified ground motions considered to be realistic for the site in question are used to generate the calculated stresses. In the cyclic triaxial test, the magnitude of principal stresses may be varied to match those expected in the field, but the principal stresses can only act in a vertical or horizontal direction. Although the direction of the maximum principal stresses may be reversed (i.e., from vertical to horizontal), no other reorientation is possible even as a transient state. Maximum shear stress is applied to only one set of orthogonal planes and other planes which may be weaker are subjected to lower shear stress. Consequently, the measured shear strength and indicated stability may be too high. During an earthquake, principal stress directions may vary randomly and any plane may be subjected to the maximum shear stress. For this and other less important reasons, material response measured in the cyclic triaxial test and used in liquefaction analyses must be corrected using empirical correction factors to match field behavior and alternative tests to more closely match field response have long been sought.

3. If the ground surface and all subsurface layers at a site are horizontal and it is assumed that most of the deformation occurring during an earthquake may be attributed to the vertical propagation of shear waves from underlying layers, then prior to the earthquake there is no shear stress on the horizontal plane and during the earthquake normal stress on the horizontal plane remains constant while the plane is subjected to cyclic shear stresses.

These assumptions are rarely satisfied in actuality. A laboratory test which simulates this highly idealogical condition is the cyclic simple shear test. An investigation by Peacock and Seed (1967) compared results from cyclic triaxial tests with those obtained from cyclic simple shear tests. The device used to perform tne tests accepted a 2- by 2- by 3/4-in.* specimen and was patterned after an original design by Dr. K. H. Roscoe of Cambridge University (1953). It was concluded from the investigation that cyclic stresses causing liquefaction under cyclic simple shear conditions were about 50 percent of those determined by corresponding cyclic triaxial test procedures. Partial development of shear stresses occurred on the vertical sides of the specimens and small voids formed at the corners produced nonuniform density and stress conditions within the specimens, however, the effects of these limitations were estimated in the development of the 50 percent correction factor. Most design procedures based on cyclic triaxial test results assume level ground conditions and use a correction factor of approximately 50 percent developed mainly as a result of this investigation.

4. The cyclic simple shear test has several disadvantages. Significant deficiencies are that maximum rotation of major principal stress direction is limited to approximately $\pm$ 4 deg and the test is subject to nonuniform stress conditions as has been found by many investigators including Wright, Gilbert, and Saada (1978). It is apparent that an alternative test is desirable to investigate effects of principal stress rotation on cyclic shear strength and to encompass the possible range of field behavior. Wright, et al. (1978) have suggested that tests on long, thin, hollow cylinder specimens with the same internal and external pressure and to which both axial force and torque may be applied will provide much better internal stress distribution than exists in simple shear specimens. By using long specimens, end effects are minimized and by using thin walled specimens, there is a more uniform radial distribution of shear stress and better definition of average shear strains are obtained. In the test developed herein, major principal planes may also be inclined at any desired angle by using the proper combination of instantaneous axial force and torque amplitudes. If such tests could be modified to provide for cyclic variation of axial force and torque with controlled phase differences between the two, then systematic, cyclic rotation of major principal

* A table of factors for converting U. S. customary units of measurements to metric (SI) units is presented on page 3.

stresses could be achieved, the effect of such rotation on the dynamic shear strength of saturated sands could be investigated, and a better understanding of the laboratory to field correction factor used in geotechnical earthquake engineering could be obtained.

5. Assume that a laboratory test can be designed and the required hardware fabricated which will allow complete and cyclic rotation of the principal stress planes and assume further that this test is the hollow cylindrical triaxial test with equal inside and outside pressure. The relationships among selected specimen dimensions will conform to those proposed by Wright, Gilbert, and Saada (1978) in order that maximum stress uniformity might be achieved.

6. The reference axes for the proposed development are shown in Figure 1a and an element under a general state of stress is shown in Figure 1b.

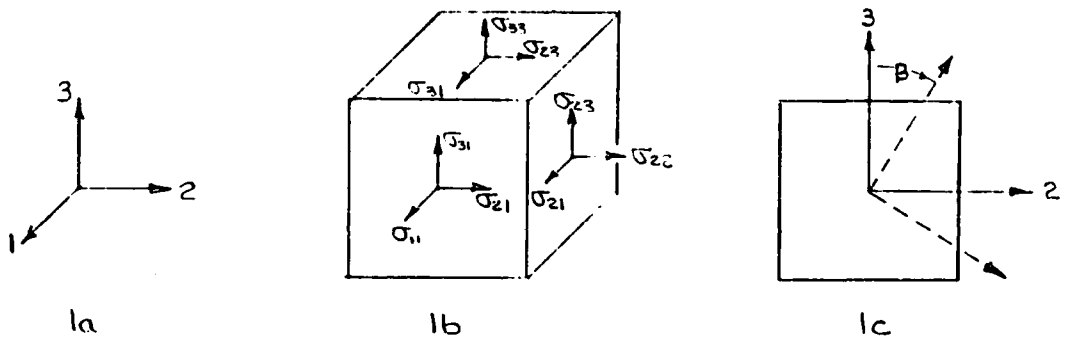

Figure 1. Reference axes and stress system

Since the inside and outside pressures on the hollow cylinder are equal, at a given point the radial and tangential stresses are equal (i.e., $\sigma_{11} = \sigma_{22}$) and do not vary with radius. The stress state reduces, effectively, to a two-dimensional stress state. For this two-dimensional case, the maximum and minimum stresses will always be in the 2-3 plane. The angle of principal stress inclination β and the stresses are related by the equation

$$\text{Tan } 2\beta = \frac{2\Delta\sigma_{23}}{\Delta\sigma_{33} - \Delta\sigma_{22}} \qquad (1)$$

where the angle β is as shown in Figure 1c. In the test proposed, the cell

pressure σ_{22} will be held constant so that

$$\text{Tan } 2\beta = \frac{2\Delta\sigma_{23}}{\Delta\sigma_{33}} = \frac{\text{Sin } 2\beta}{\text{Cos } 2\beta} = \frac{K \text{ Sin } 2\beta}{K \text{ Cos } 2\beta} \tag{2}$$

where

β = the angle of principal stress inclination

K = the maximum principal stress difference. It is an independent variable selected prior to testing and always occurs in the 2-3 plane. K is equivalent to σ_{dc} in the cyclic triaxial test and when $\Delta\sigma_{23}$ is reduced to zero, β becomes zero, a requirement in the cyclic triaxial test.

Equation 2 may be separated into two equations

$$\Delta\sigma_{23} = \frac{K}{2} \text{ Sin } 2\beta \tag{3}$$

$$\Delta\sigma_{33} = K \text{ Cos } 2\beta \tag{4}$$

which indicates that if an harmonic axial stress increment σ_{33} is applied to a hollow cylindrical specimen along with a syncronized harmonic shear stress $\Delta\sigma_{23}$ in such a manner that Equations 3 and 4 are satisfied simultaneously, then the principal stress planes inclined at angle β will rotate cyclically and continuously. The snear stress increment ($\Delta\sigma_{23}$) and axial stress increment ($\Delta\sigma_{33}$) must be applied as shown in Figure 2.

7. The cyclic change in state of stress in the proposed system reduces to

$$\begin{vmatrix} \Delta\sigma_{11} & \Delta\sigma_{21} & \Delta\sigma_{31} \\ \Delta\sigma_{21} & \Delta\sigma_{22} & \Delta\sigma_{23} \\ \Delta\sigma_{31} & \Delta\sigma_{23} & \Delta\sigma_{33} \end{vmatrix} = \begin{vmatrix} 0 & 0 & 0 \\ 0 & 0 & \Delta\sigma_{23} \\ 0 & \Delta\sigma_{23} & \Delta\sigma_{33} \end{vmatrix} \tag{5}$$

The total stress tensor for the stress system under consideration is

$$\begin{vmatrix} \sigma_{11} & \sigma_{21} & \sigma_{31} \\ \sigma_{21} & \sigma_{22} & \sigma_{23} \\ \sigma_{31} & \sigma_{23} & \sigma_{33} \end{vmatrix} = \begin{vmatrix} (\bar{\sigma}_3 + \sigma_{BP}) & 0 & 0 \\ 0 & (\bar{\sigma}_3 + \sigma_{BP}) & (\Delta\sigma_{23}) \\ 0 & (\Delta\sigma_{23}) & (\bar{\sigma}_3 + \sigma_{BP} + \Delta\sigma_{23}) \end{vmatrix} \tag{6}$$

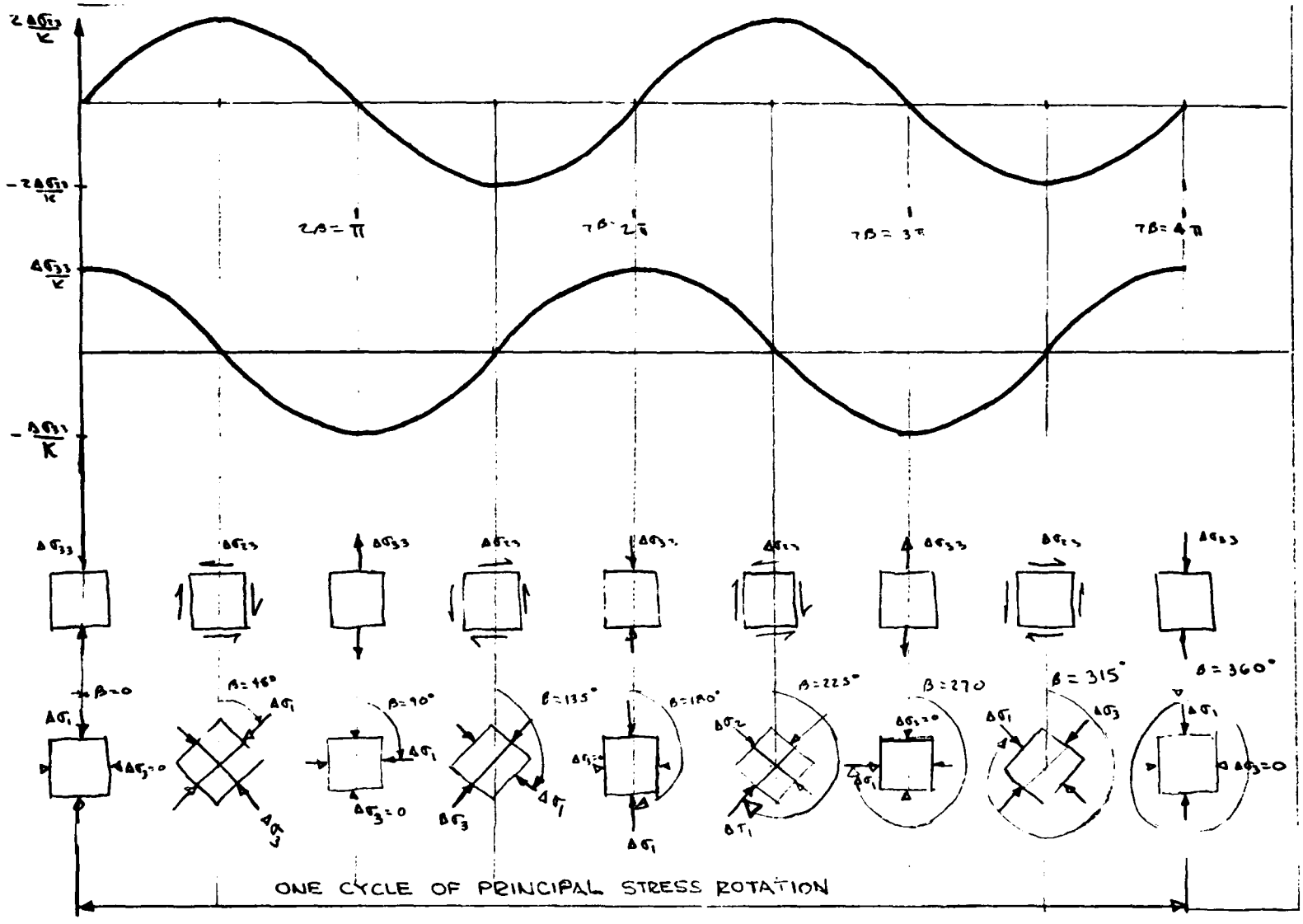

Figure 2. Synchronization of axial and shear stress for principal stress rotation

where

$\bar{\sigma}_3$ = the initial effective confining pressure

σ_{BP} = the applied back pressure

The effective stress tensor for the system is

$$\begin{vmatrix} \sigma_{11} & \sigma_{21} & \sigma_{31} \\ \sigma_{21} & \sigma_{22} & \sigma_{23} \\ \sigma_{31} & \sigma_{23} & \sigma_{33} \end{vmatrix} = \begin{vmatrix} (\bar{\sigma}_3 - \Delta u) & 0 & 0 \\ 0 & (\bar{\sigma}_3 - \Delta u) & (\Delta\sigma_{23}) \\ 0 & (\Delta\sigma_{23}) & (\bar{\sigma}_3 + \Delta\sigma_{33} - \Delta u) \end{vmatrix} \tag{7}$$

where

Δu = the induced pore water pressure

8. It should be noted that in position $2\beta = \pi, 2\pi \ldots, n\pi$ it appears that the specimen is in tension. Of course, it is not because the initial effective confining pressure, which is compressive, is a superposed normal stress at all positions of loading. The cohesionless specimen can not withstand tensile stresses, therefore exactly as in the cyclic triaxial test, the value of K must be selected such that

$$\frac{K}{\bar{\sigma}_3} \leq 1 \text{ or } \frac{K}{2\bar{\sigma}_3} \leq \frac{1}{2} \tag{8}$$

or else direct tension will be applied to the specimen during the first cycle of loading and the specimen will fail upon application of a direct tension.

9. The principal stresses of the stress system of Equation 5 are determined by solving the characteristic equation. The principal stresses for this state of stress are:

$$\Delta\sigma_1 = \frac{\Delta\sigma_{33}}{2} + \sqrt{\frac{\Delta\sigma_{33}^2}{2} + \Delta\sigma_{23}^2} \tag{9}$$

$$\Delta\sigma_2 = 0 \tag{10}$$

$$\Delta\sigma_3 = \frac{\Delta\sigma_{33}}{2} - \sqrt{\frac{\Delta\sigma_{33}^2}{2} + \Delta\sigma_{23}^2} \tag{11}$$

and

$$\Delta\sigma_1 = \frac{K}{2} [\text{Cos } 2\beta + 1] \tag{12}$$

$$\Delta\sigma_3 = \frac{K}{2} [\text{Cos } 2\beta - 1] \tag{13}$$

Using this approach, the shear stress and axial stress applied to the hollow cylinder are sinusoidal in nature and 90 deg out of phase. The required shear stress will be produced by applying torsion to the hollow cylinder and the specimen wall must be thin enough that the tangential moment, and hence the shear stress, does not vary appreciably over the cross section of the specimen.

10. The stress K determines the intensity of loading for any one test, and when chosen will determine the magnitude of $\Delta\sigma_{23}$ and $\Delta\sigma_{33}$, as seen from Equations 3 and 4.

11. Some interesting observations may be made about this stress system. It is evident that the principal stresses do rotate continuously and completely as expressed by the angle β seen in Equation 2. Also, the size of the Mohr's circle of stress in two dimensions, $\Delta\sigma_1 - \Delta\sigma_3$, once applied is never changed. It maintains its size throughout cyclic loading in terms of effective or total stresses. The position of the Mohr's circle, however, shifts as the angle β changes in total stress space as shown in Figure 3.

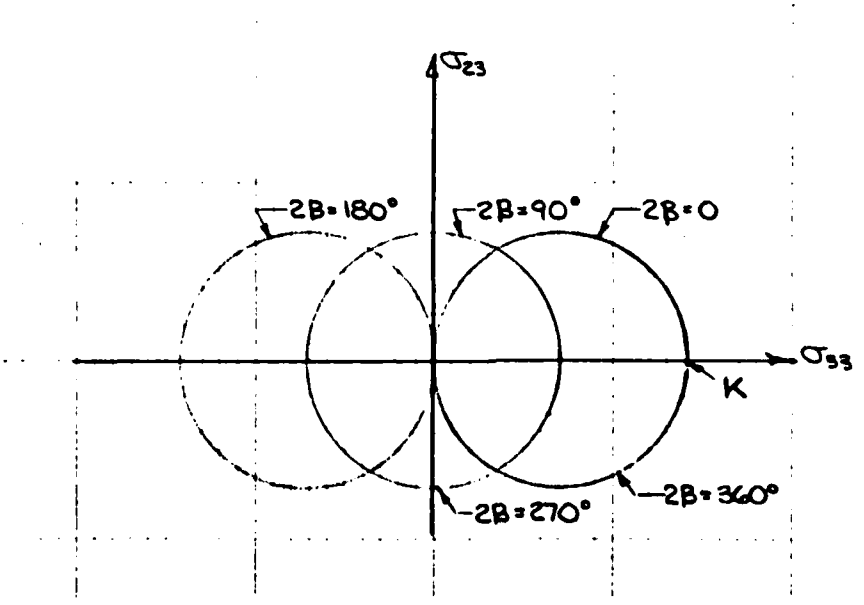

Figure 3. Mohr's circle shifts as angle β changes

In effective stress space, the shift of the Mohr's circle will be dictated by the buildup of pore water pressure, but the net shift will always occur in the direction toward the Mohr's strength envelope (Figure 4). Therefore, with enough cycles of intense enough loading, a specimen can be expected to approach 100 percent pore pressure response and instability; the number of principal stress rotations to this condition is both material and stress dependent.

12. The purposes of this investigation are to develop a hollow cylinder testing device which may be used to provide cyclic rotation of major principal stresses and to conduct a preliminary testing program to investigate the effects of cyclic rotation of principal stresses in cyclic strength tests to determine liquefaction susceptibility.

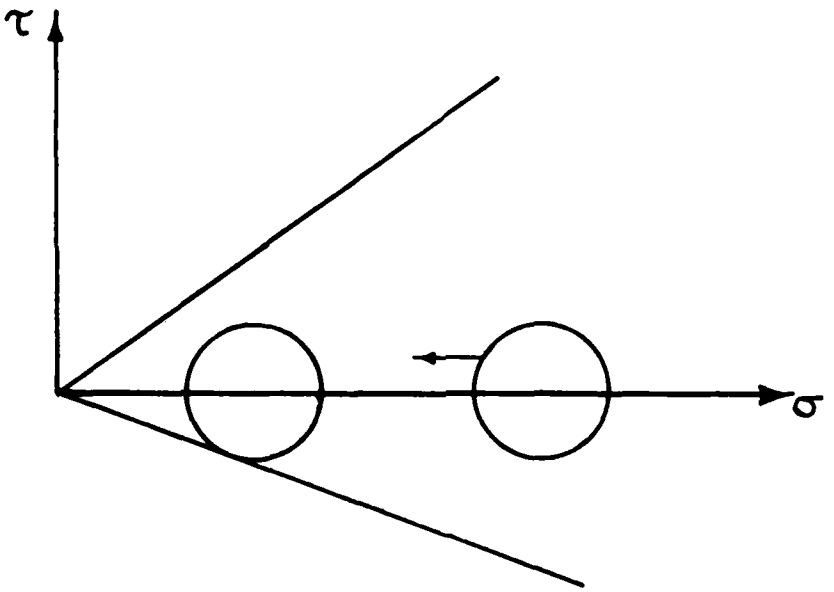

Figure 4. Direction of travel of Mohr's circle based on effective stresses

PART II: TESTING APPARATUS

13. A testing apparatus that met the requirements for hollow cylinder principal stress rotation testing was designed and fabricated at WES. This apparatus is a modification of the static hollow cylinder test device reported by Saada (1967). A photograph of the new WES apparatus, including electronic controls, pneumatic pressure control devices, and the data acquisition system is shown in Figure 5. The apparatus accepts a hollow cylinder specimen, 8.0 in. high with an outside diameter of 4.0 in. and an inner diameter of 2.8 in. The specimen is encased within 0.012-in.-thick rubber membranes (inner and outer) between a rigid cap and base. Fluid pressure acts on the inner and outer surfaces of the specimen to produce the minor principal stress. The axial load piston is rigidly attached to the specimen cap so that the axial force may be cycled in both compression and extension and also so that torque may be applied to the specimen. Descriptions of various components of the apparatus are given in the following sections.

Electro-Pneumatic Cyclic Loading Systems

14. Pneumatic actuators are used to apply cyclic axial force and cyclic torque to the specimen according to the desired loading wave forms. Cyclic pressures supplied to the actuators are produced by Fairchild Model T 5121D current to pressure transducers manufactured by Fairchild Industrial Products Division in Winston-Salem, North Carolina. The electric current supplied to the transducers is controlled by an MTS Model 410 function generator manufactured by MTS Systems Corporation of Minneapolis, Minnesota. The function generator provides two output voltages that vary sinusoidally with time and are 90 deg out of phase. The outputs of the function generator are converted to desired current amplitudes by Hewlett Packard Model 6824A DC power amplifiers.

Axial loading system

15. A schematic diagram of the axial loading system is given in Figure 6. The axial force actuator has a 7.8-in.-diam bidirectional piston equipped with a rolling diaphragm seal to minimize friction. Cyclic axial forces are applied to the specimen by varying the pressure acting on top of the piston in the actuator. The pressure is supplied by a Kendall Model 15

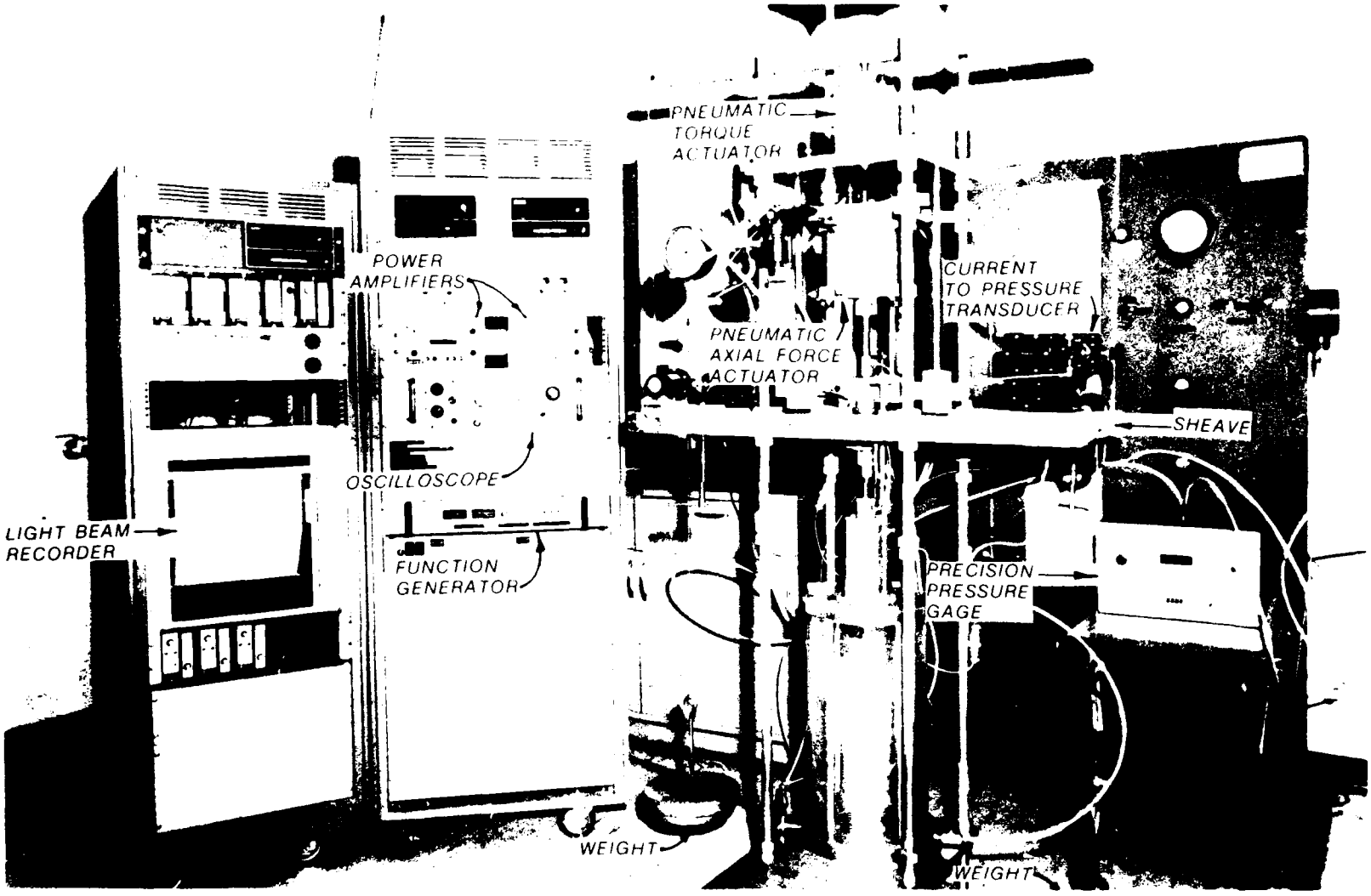

Figure 5. Hollow cylinder principal stress rotation testing apparatus

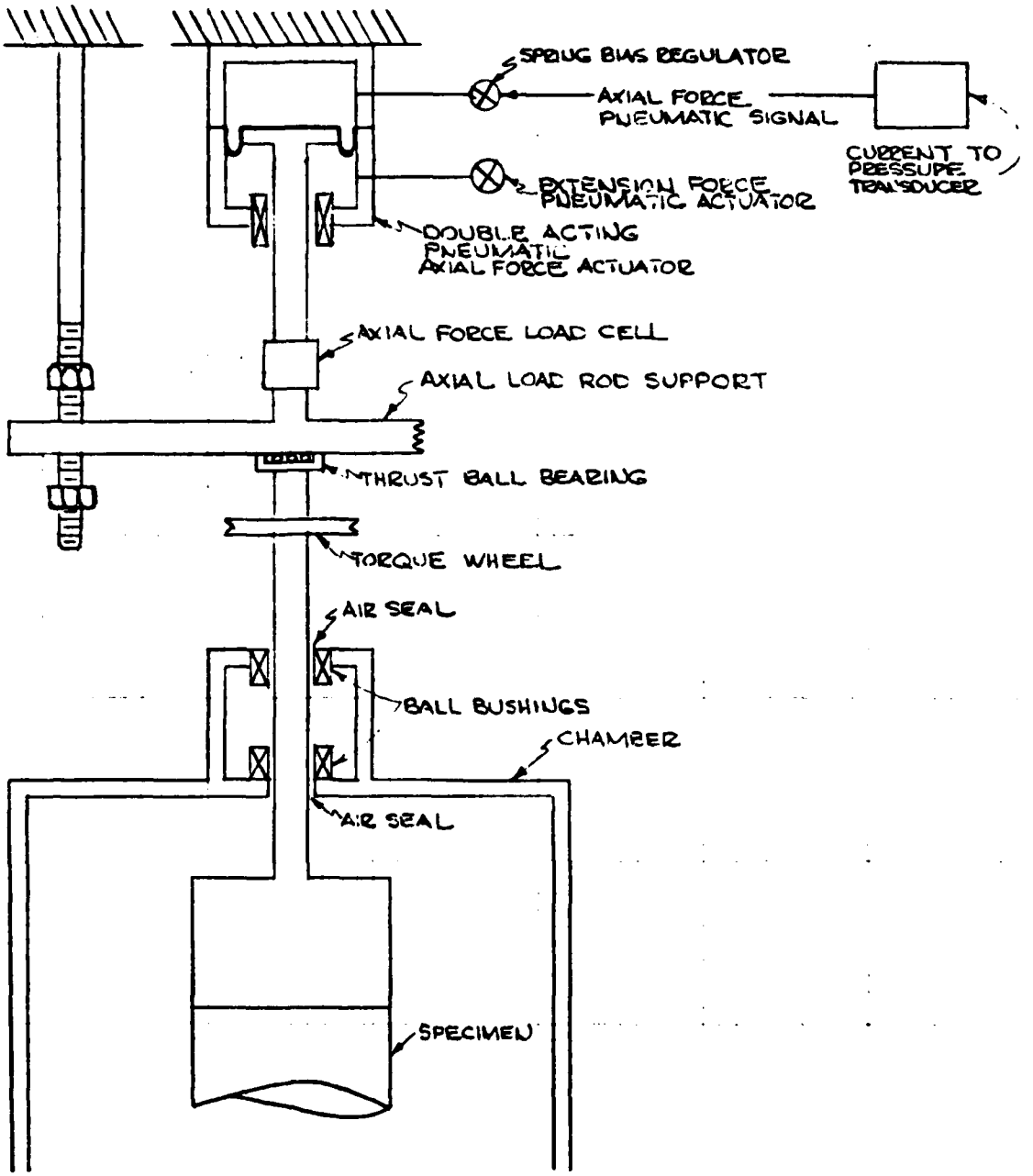

Figure 6. Schematic diagram of axial loading system

spring bias booster relay attached to the load frame. The relay provides an output pressure which is a function of signal pressure plus a set bias. In this case the set bias is used to supply a pressure equal to the pressure in the bottom of the actuator plus that required to counteract the uplift force due to the chamber pressure. The signal pressure is the cyclic pressure supplied by the current to pressure transducer. Prior to a test, sufficient pressure is added to the bottom of the actuator to produce the maximum desired axial force during the extension portion of the cycle. This pressure is held constant during the test. The axial force is measured by a Transducers Inc. Model WML 2-251-500 miniature load cell located immediately above the axial load rod support. The load rod support consists of a cross bar rigidly attached to the piston with holes at each end through which threaded vertical rods pass. Nuts on the rods are used to raise or lower the piston and to lock it into place. The housing at the top of the chamber contains an air-seal to minimize friction occurring as the piston enters the chamber and linear ball bushings to prevent lateral movement of the piston. Piston friction in the loading system is negligible for linear as well as rotary motion.

Torque loading system

16. A schematic diagram of the torque loading system is shown in Figure 7. Torque is transmitted to the torque wheel on the loading piston by cables to a cross bar attached to the piston of a pneumatic actuator and to a pair of matched weights of weight W. Prior to starting a test, sufficient pressure is supplied to the actuator to nullify the torque applied by the weights. The cables supporting the weights are then clamped to bars attached to the load frame between the sheaves and the torque wheel. As in the case of the axial load actuator, pressures are supplied to the actuator by a Kendall Model 15 spring bias booster relay. In this case though, the set bias is the pressure required to nullify the torque applied by the weights and the signal pressure is the cyclic pressure supplied by the current to pressure transducer. Torque is applied to the specimen in a counterclockwise direction (viewed from the top) when the pressure in the actuator is sufficient to lift the weights from the null position and in a clockwise direction when the pressure is insufficient to obtain the null position. There is approximately 90 deg of twist available in both directions from the null position. Forces applied to the torque wheel are measured by Transducer Inc. Model WML 2-251-200 miniature load cells attached to the cables to the actuator. A thrust ball bearing

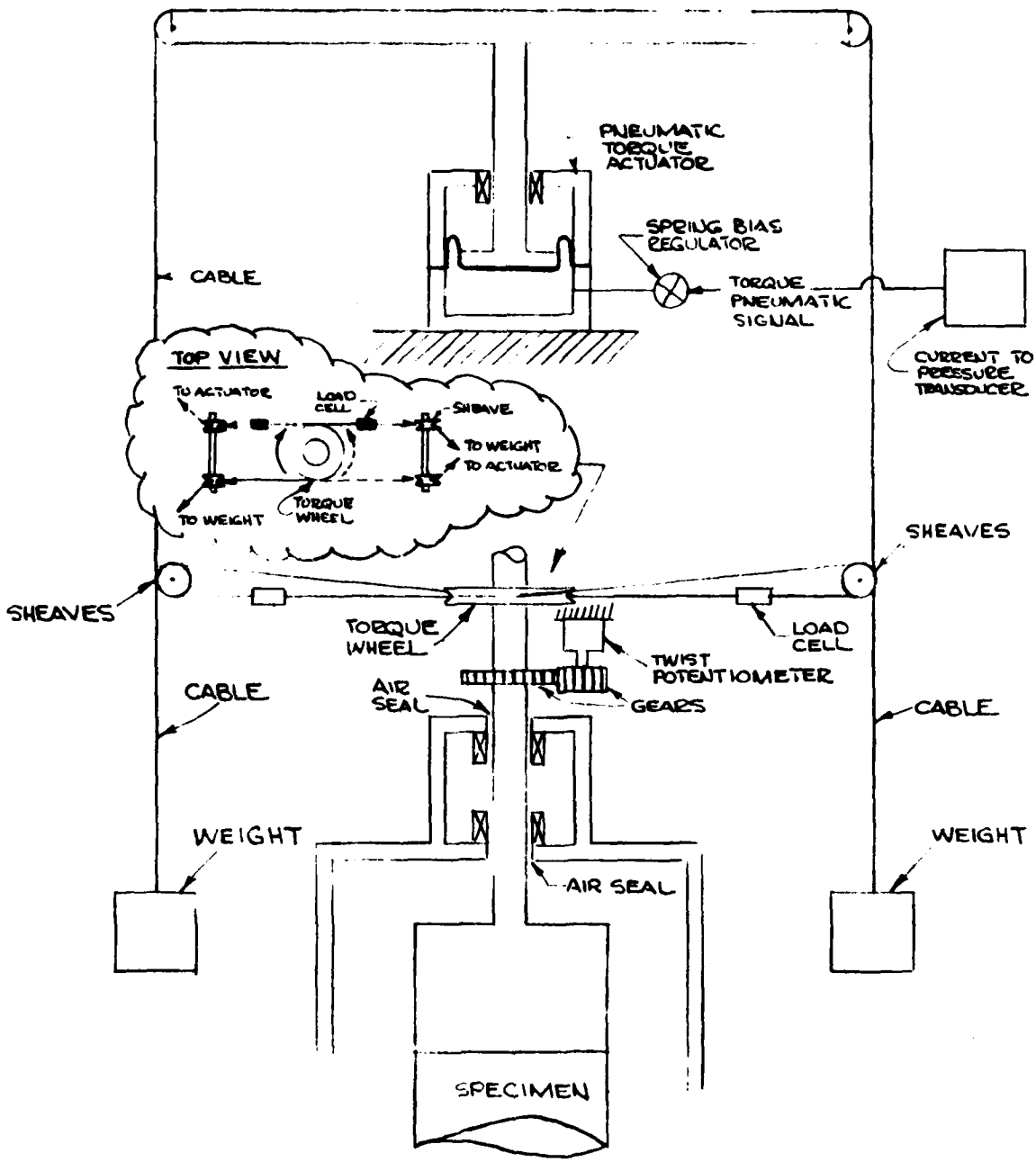

Figure 7. Schematic diagram of torque loading system

connected to the bottom of the axial load rod support bar allows the loading piston to rotate when the piston is in either compression or extension. Friction in the torque loading system was found to be negligible when the sheaves between the torque wheel and the actuator and weights were vibrated slightly during loading of the specimen.

Specimen Deformation and Pore Pressure Measuring Devices

17. Axial deformation was determined by measuring the vertical movement of the axial load rod with a linearly variable differential transformer (LVDT). The LVDT was calibrated to measure deformations to within $\pm$ 0.0001 in. Rotational deformation of the specimen cap (twist) was measured by a potentiometer connected to the shaft of a gear which was driven by a larger gear on the loading piston (see Fig. 7). The potentiometer was calibrated to measure rotational deformation of the cap to the nearest 0.1 deg. Specimen pore water pressure was measured external to the specimen with a CEC pressure transducer connected via a drainage line to the porous stone in the base (specimen pedestal). The transducer was calibrated to measure the pressure to the nearest 0.1 psi.

Data Acquisition System

18. Outputs from the various electronic sensors were monitored by Doric Model DS-100 integrating microvoltmeters and recorded during loading by a Honeywell Model 1912 light beam strip chart recorder.

Cap and Base

19. The hollow cylinder specimen cap and base were fabricated from aluminum and were equipped with sintered stainless steel, annular-shaped plates on which the specimen rested. Single-edge razor blades were cemented into the plates at 45-deg intervals to aid in transferring torsional stresses to the specimen. The blades protruded approximately 0.1 in. from the surfaces of the plates. Figure 8 is a bottom view of the lower portion of the specimen cap showing an annular plate and blades. (A top view of the specimen base may be seen in Figure 12.) Figure 9 shows a top view of the lower portion of the cap

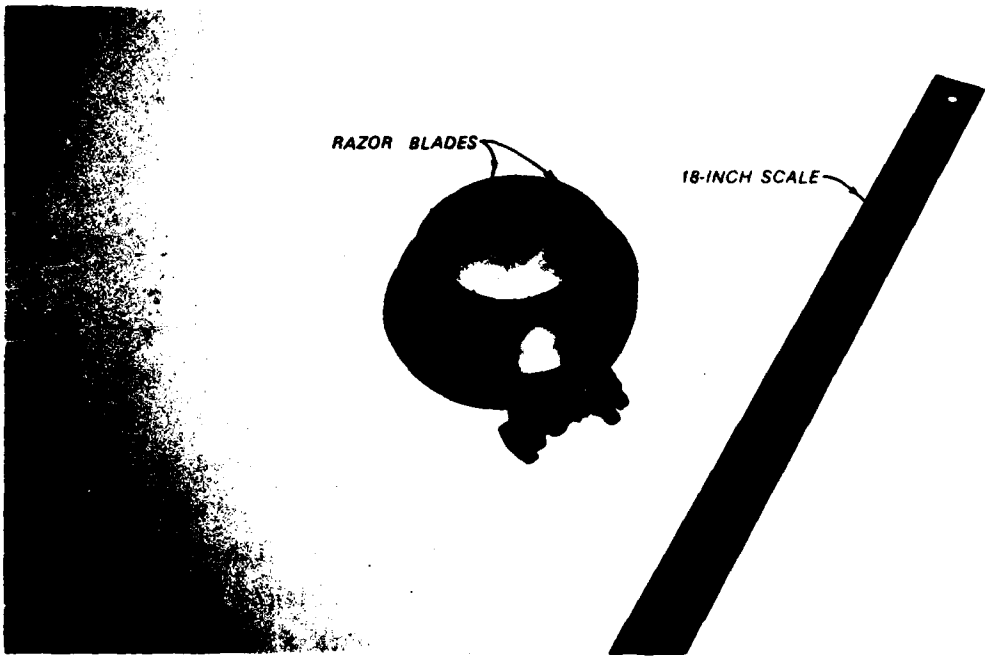

Figure 8. Bottom view of lower portion of specimen cap

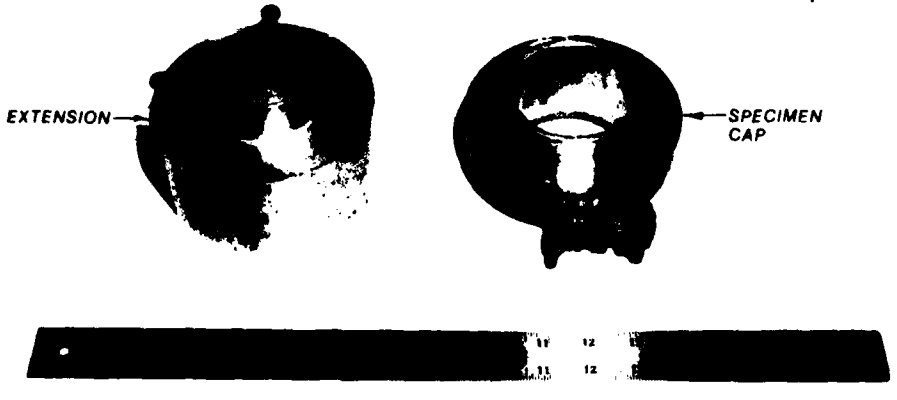

Figure 9. Top view of lower portion of specimen cap and extension for transferring torque and axial force to specimen

and the extension for transferring torque and axial force to the specimen (the lower end of the loading piston fits into the square opening in the extension where it is locked in place using set screws). The extension is attached to the specimen cap with four screws. Specimen drainage was provided from both the cap and the base.

Chamber

20. Figure 10 shows the test chamber containing a hollow cylinder specimen. The major components of the chamber are: a fixed aluminum base with a flange containing an "O" ring and ports to which chamber pressure and specimen drainage lines may be connected; three stainless steel vertical alignment rods; an aluminum plate with an "O" ring groove and "O" ring on its top surface; a loading piston guide housing; a lucite cylinder; and a ring flange containing an "O" ring. The chamber is assembled by screwing the steel rods into the base and attaching the alignment plate (which has a diameter slightly smaller than the lucite cylinder) and loading piston housing to the top of the rods. The lower end of the loading piston is then placed into the specimen cap extension and secured with set screws. The benefit of having alignment rods inside the chamber is that the locking of the loading piston and adjustments required to assure proper alignment may be made without interference from the lucite cylinder. After placing the lucite cylinder over the alignment plate and pushing it into the base, the ring flange is pushed over the top of the cylinder and secured with hand knobs. The cylinder is sealed on its outside surface by the "O" rings in the base and ring flange. The top of the chamber is sealed by the "O" ring on the slignment plate acting against the bottom surface of the ring.

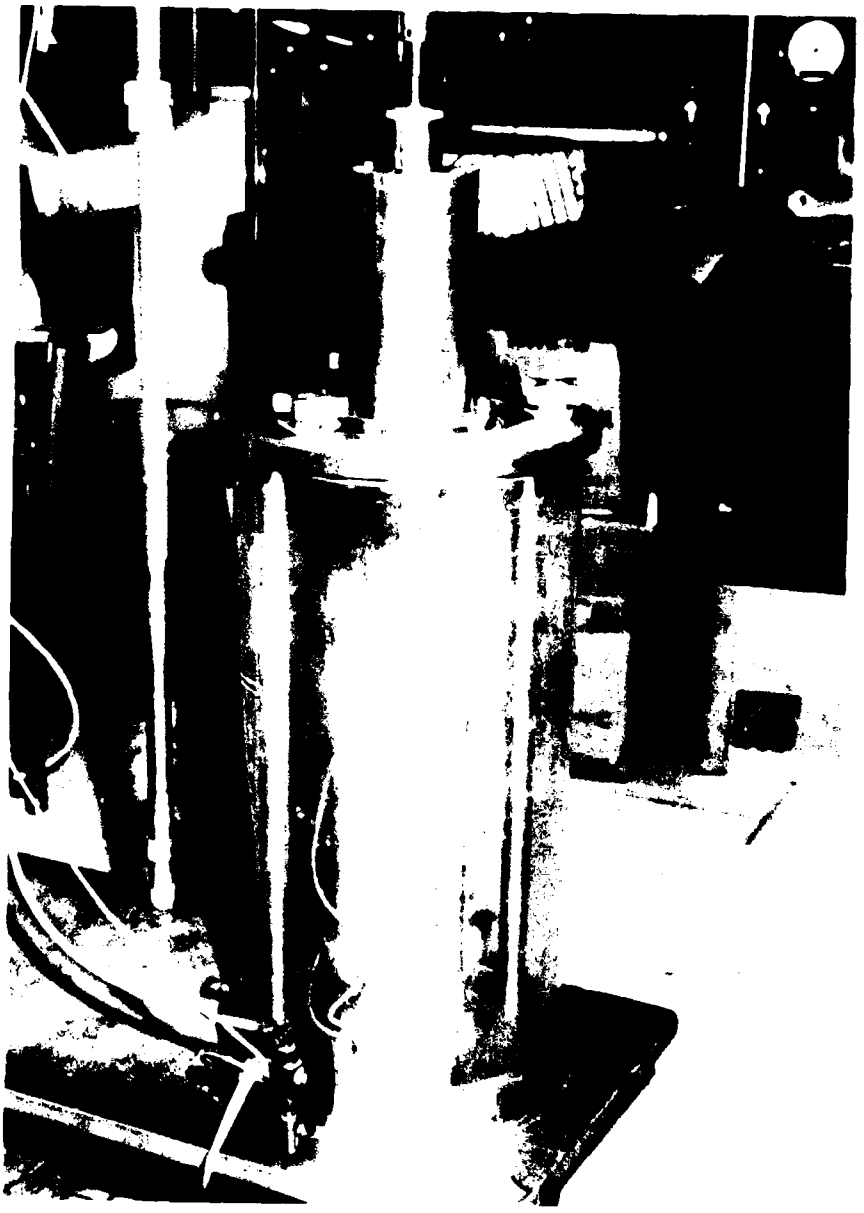

Figure 10. Test chamber

PART III: SPECIMEN PREPARATION

Material

21. The performance of the new hollow cylinder testing device was evaluated by performing five consolidated-undrained principal stress rotation tests on saturated specimens of Monterey No. 0 sand at a relative density of 50 percent. Monterey No. 0 sand was chosen for this purpose because it nas been used in investigations involving both cyclic triaxial and cyclic direct simple shear tests. The material was obtained from the Lone Star Sand Company in Monterey, California. The gradation, specific gravity, and relative density parameters of Monterey No. 0 sand are given in Figure 11.

Specimen Mold

22. The mold in which specimens were compacted consisted of a four-piece split mandrel inside a two-piece split mold. Figures 12 through 16 show how the mold was assembled prior to compacting a specimen. After placing the inner 0.012-in.-thick membrane over the bottom of the specimen base and sealing it with a rubber O-ring, the parts of the mandrel were placed inside the membrane (Figure 12) formed into a cylinder resting in a receptacle in the base. The inner membrane was then pulled up around the mandrel and the top forming ring was fastened in place to maintain the cylindrical shape of the mandrel (Figure 13). The lateral support rod was then placed through the hole in the forming ring and screwed into the base of the chamber (Figure 14). A nut on the rod was then screwed tightly against the forming ring to hold the mandrel rigidly in place (Figure 15). After the outer 0.012-in.-thick membrane was pulled over the base and sealed with an O-ring, the two-piece mold was placed around the base and secured with a hose clamp. The membrane was then pulled over the top of the mold and a vacuum was applied through a hole in the mold to draw the membrane against the inner surface of the mold (Figure 16).

Specimen Compaction

23. Specimens for the evaluation tests were compacted to a relative

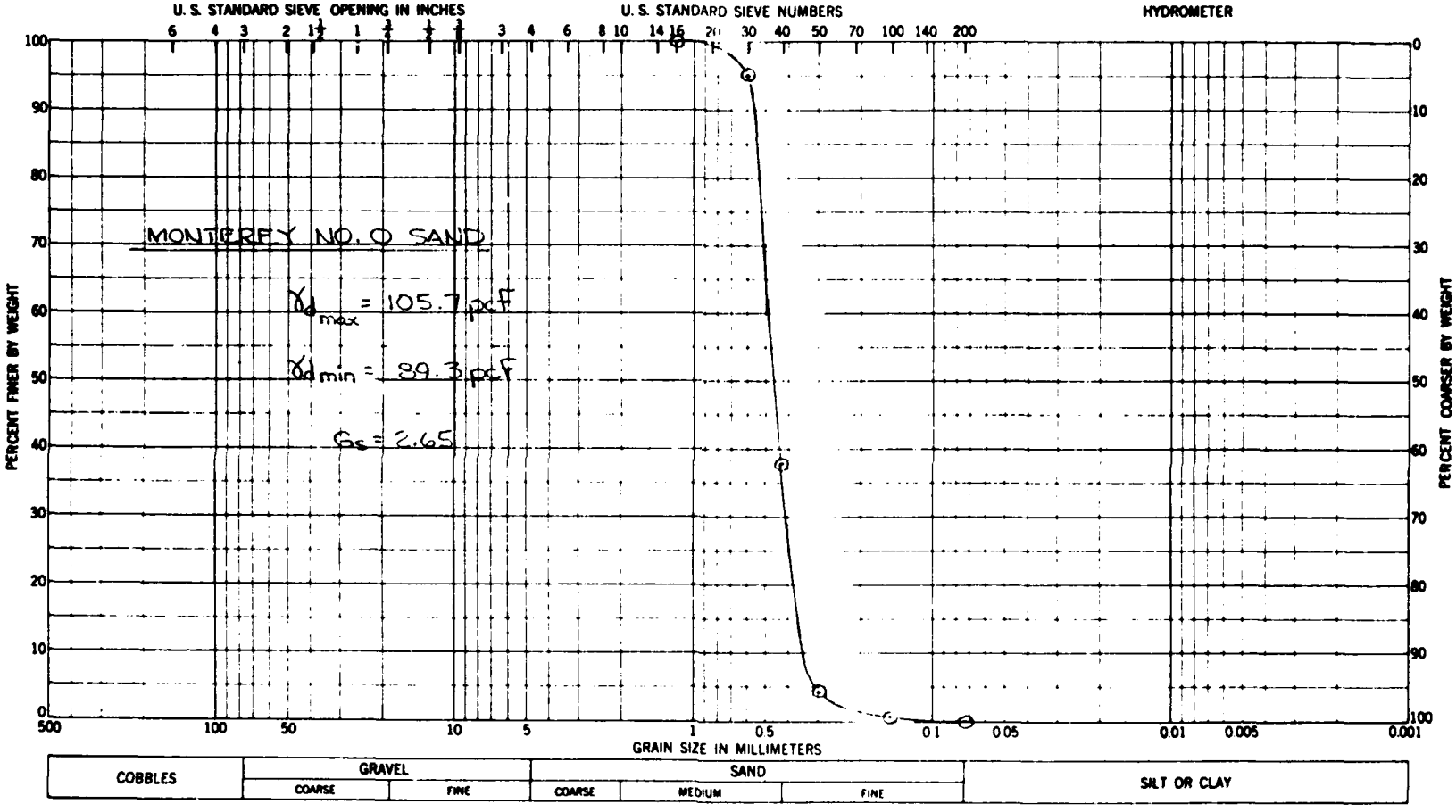

Figure 11. Gradation, specific gravity, and relative density parameters of Monterey No. 0 sand

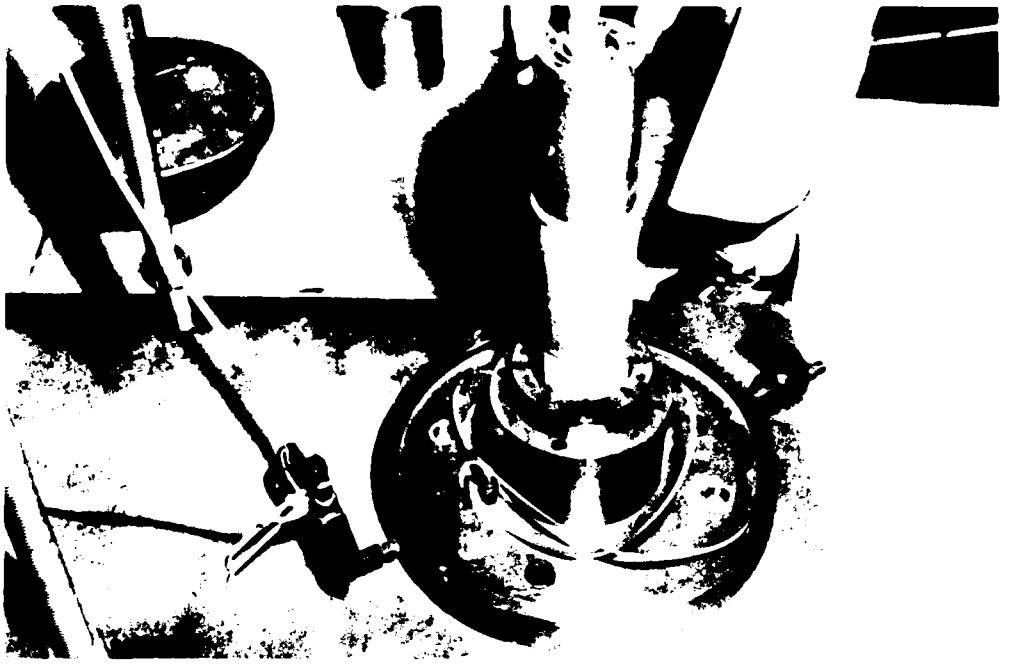

Figure 12. Placing parts of mandrel inside inner membrane

Figure 13. Fastening the forming ring to maintain the cylindrical shape of the mandrel

Figure 14. Fastening the lateral support rod to the chamber base

Figure 15. Securing the alignment of the mandrel

Figure 16. Assembled hollow cylinder specimen mold

density, D_d , of 50 percent using a moist tamping method. The molding water content was 8.0 percent. Specimens were compacted in six layers using the tamper shown in Figure 16; for each layer, preweighed amounts of soil were placed in the mold. With the exception of the last layer, each layer was compacted to a surface elevation calculated to yield the desired relative density using calibrated marks on the tamper as a guide. The last layer was tamped to within approximately 0.2 in. of the desired height using the tamper and then compacted to the desired density by placing the specimen cap in position on the specimen and tamping the top of it until the desired height was achieved. This was done to assure proper seating of the cap on the specimen. The top of each layer was scarified prior to adding material for the next layer. In order to avoid overcompaction of the lower layers, the weight of material for each layer was varied so that the bottom layer was initially compacted to a relative density of 47 percent and each succeeding layer was initially compacted to a relative density one percentage point higher than the preceding one, assuming no further densification of underlying layers. Following compaction the inner and outer membranes were pulled over the specimen cap and sealed with rubber O-rings. A partial vacuum of - 10.0 psi was then applied to the specimen through the drainage line to the specimen base and the mold was dissassembled. Measurements were then made to determine the specimen dimensions.

PART IV: TEST PROCEDURE

Preparation of Equipment

24. After obtaining the specimen dimensions following compaction, the chamber was assembled and moved under the load frame. The adapter on the end of the upper portion of the axial load piston (located under the twist indicator) and the portion of the piston leading to the specimen cap were carefully aligned and locked into position. Prior to locking the piston in place, nuts on the axial load piston support bar were positioned to support the weight of the upper part of the piston and to locate the piston so that sufficient travel would be available for approximately $\pm$ 10 percent axial strain during cyclic loading. The torque wheel remained locked in place at its null position during this part of the procedure. The chamber was then filled with deaired water to within 0.5 in. of its top (the annular volume of the specimen was completely filled during this process). An air pocket was required at the top of the chamber to keep water out of the air seal and to avoid fluctuations in chamber pressure due to the piston moving in and out of the chamber during cyclic shear. Although the air pocket exposed a large surface area on which the chamber pressure could act to place air into solution, the total time to complete a test was short enough so that there should be no problems due to air diffusing through the membranes.

Saturation

25. Saturation of the specimens was accomplished by first using vacuum to remove air from the specimen and specimen drainage system (including lines, porous end platens, and pore water pressure measurement system) and then allowing desired water to percolate from the bottom to the top of the specimen under a low differential vacuum head (> 3.0 psi). This was followed by the use of back pressure to place remaining air into solution. Prior to compacting a specimen, the drainage lines to the specimen and the porous end platens were dried in order to remove water which might contain significant amounts of air in solution. The maximum vacuum applied to specimens to evacuate air during the first stage of saturation was the 10.0 psi partial vacuum used to support the specimens after compaction. Back pressures required to achieve

saturation ranged from 20 to 40 psi. Specimens were considered to be saturated if Skempton's "B" parameter values exceeded 0.95. Skempton's "B" parameter is defined as the ratio of the measured increase in induced pore pressure to an increase in chamber pressure with the specimen drainage valves closed. The axial force was increased when the chamber pressure was increased during back pressuring to maintain an isotropic stress condition on the specimen. During back pressuring, the difference between the chamber and back pressure was maintained at 5.0 psi.

Consolidation

26. All of the specimens were consolidated under an isotropic effective confining pressure of 14.22 psi (1.0 kg/cm^2) after back pressure saturation. This was accomplished by increasing the chamber pressure by 9.22 psi (resulting in an effective confining pressure of 14.22 psi or 1.0 kg/cm^2) and increasing the axial force an appropriate amount to maintain an isotropic condition. During consolidation the specimen height and volume change were monitored by means of the LVDT and a burette. When the LVDT and burette indicated no further change in volume due to the increase in confining pressure, the specimen drainage valves were closed and the pore pressure was observed. If there was no change in pore pressure for a period of 10 min after the specimen drainage valves were closed, consolidation was assumed to be completed. The time for the consolidation phase of each test was approximately 2 hr.

Cyclic Shear

27. Following consolidation the axial load support bar was locked in place and the electropneumatic loading systems were adjusted to provide the required cyclic axial force and torque. Since the axial load piston and torque wheel were locked in place, the axial force and torque could be applied to the measuring devices (load cells) and adjusted without being applied to the specimen, thus assuring that the desired force and torque amplitudes for the test were achieved. After the cyclic loading amplitudes were set, the forces required to maintain the null position on the torque wheel and the isotropic stress condition on the specimen were checked and readjusted if necessary. The locking devices were then disconnected and a short period of

time was allowed to lapse so that the specimen could recover equilibrium in case there was any slight disturbance during the calibration phase. Finally, the specimen drainage valves were closed and cyclic loading of the specimen was initiated at a rate of one complete rotation of principal stresses every 66 sec.

28. As described in paragraph 14, a sine wave loading form was used for both torque and axial force. The wave forms were 90 deg out of phase to provide for a complete rotation of the major principal planes during each loading cycle. A typical test record for a loading cycle is given in Figure 17. As may be seen, outputs from the axial force load cell, the summed and averaged torque load cell readings, the axial deformation LVDT, the twist or angular deformation potentiometer, and the pore water pressure transducer were recorded during cyclic loading. Note that two complete cycles of torque and axial force application are required for one complete rotation of the major principal planes.

29. Following failure of the specimen, the axial loading piston and torque wheel were locked in position at their preshear locations and a vacuum was applied to the specimen. The chamber was then removed from the loading frame and was dismantled after it was drained. The total specimen was dried to obtain its dry weight.

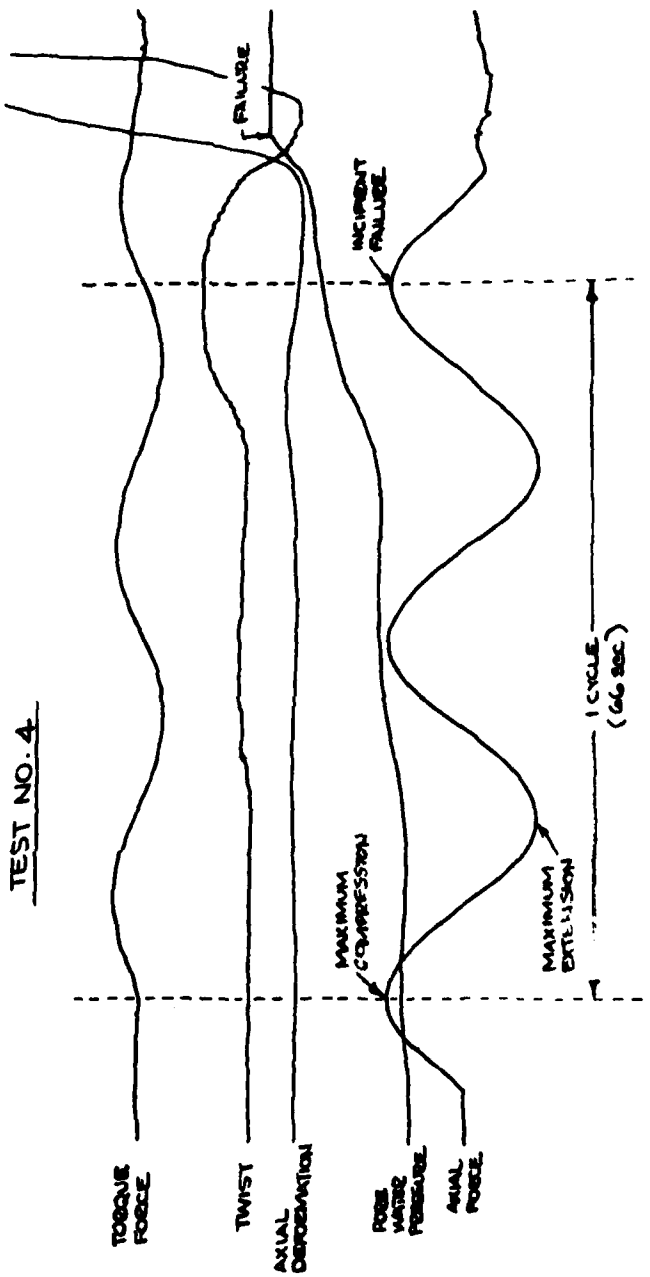

Figure 17. Example of test record

PART V: RESULTS OF PRELIMINARY TESTS

30. A total of five tests were performed in the preliminary testing program. The objective of the testing program was to evaluate the performance of the new hollow cylinder principal stress rotation device by testing specimens of Monterey No. 0 sand compacted to 50 percent initial relative density and consolidated under an isotropic effective confining pressure, σ_{3c}, of 1.0 kg/cm^2. Typical behavior during cyclic loading is given in the test record shown in Figure 17. As may be seen from the appropriate traces in this figure, axial force and torque were applied according to the desired sinusoidal wave forms and the wave forms were 90 deg out of phase. It should be kept in mind that in these tests, one complete rotation of the major principal planes subjected every plane in the specimen to a maximum shear stress equal to one-half the principal stress difference (a principal stress difference equal to the radius of the Mohr's circle) and that the shear stress on a given plane varied from zero to the maximum value and back in one direction when the specimen was in compression and varied in the same manner except in the opposite direction when the specimen was in extension. Thus the shear stress on every plane was cycled twice in two opposing directions during one complete rotation of the major principal planes (see Figure 2). One cycle of loading was taken to be one complete rotation of principal stresses. Failure in the tests is defined as the point in the test where the pore pressure equaled the chamber pressure. Incipient failure is defined as the point in the test at the peak of the last full-sized axial force stroke in compression or tension prior to failure. Table 1 summarizes test conditions at incipient failure.

Induced Pore Pressure

31. In each test, induced pore pressure gradually increased with increasing loading cycles (rotations of major principal planes) to the cycle during which failure occurred, where there was a comparatively rapid increase. The pore pressure cycled slightly in phase with the cyclic axial force as the major principal stresses were rotated during each cycle with more positive induced pore pressures occurring during compression strokes. The peak to peak variation in pore pressure prior to incipient failure averaged 0.6 psi. Since the size of the Mohr's circle did not change during loading, it would not be

Table 1

Test Conditions at Incipient Failure[1]

Test No.[2]	Cyclic Stress Ratio $K/2\sigma_{3c}$	Cycle No.[4]	Last Full Axial Force Stroke Occurred in	Axial Strain %	Cumulative Twist[5] deg	Cumulative Shear Strain Based on Twist ν_T, %	Induced Pore Pressure Δu, psi	$\Delta u/\sigma_{3c}$
1[3]	0.20	--	Compression	--	--[6]	--	--	--
2	0.09	3	Extension	-0.24	12.4	4.6	8.8	0.62
3	0.09	5	Compression	+0.09	5.6	2.1	9.1	0.64
4	0.15	1	Extension	-0.06	0.9	0.3	8.3	0.58
5	0.07	42	Extension	-0.03	17.9	6.8	11.5	0.81

NOTES:
(1) Incipient failure is defined as the point in the test at the peak of the last full-sized axial force stroke in compression or tension prior to failure
(2) All specimens were compacted to an initial relative density of 50 percent and were consolidated under a confining pressure of 1.0 kg/cm^2
(3) Specimen for Test No. 2 failed during first torque stroke
(4) One cycle is defined as one complete rotation of major principal stresses
(5) Rotation of top cap
(6) Arrows denote direction of cumulative twist as viewed from top of specimen

expected that the pore pressure would cycle as it does during cyclic triaxial or cyclic simple shear tests. As may be seen in Table 1, incipient failure occurred at ratios of induced pore pressure to confining pressure, $\Delta u/\Delta\sigma_{3c}$, ranging from 0.58 to 0.81 with the trend indicating, as is the case in other cyclic tests, that at lower stress ratios pore pressures develop more gradually.

Specimen Deformation

32. Specimen heights changed only slightly prior to the cycle in which failure occurred. From Table 1 it may be seen that axial strain values at incipient failure ranged from - 0.24 to + 0.9 percent. All but one specimen (that for Test No. 3) increased in height prior to failure. Most of the specimen deformation during cyclic loading was produced by torsional stresses, thus indicating that horizontal planes in the specimens were considerably weaker than planes at other inclinations. This probably reflects specimen anisotropy resulting from the specimen preparation procedure. As may be seen in Table 1, twist angles at incipient failure varied from 0.4 to 17.9 deg and shear strain values based on the twist angles ranged from 0.2 to 6.8 percent. The strain values were computed using the following equation:

$$\gamma, \% = \frac{Rm\ \theta}{L} \times 100 \qquad (14)$$

where

γ = shear strain expressed as a percentage

Rm = mean radius of specimen in inches

$= 4/3\ \frac{R^3 - r^3}{R^2 - r^2}$ where R and r are the outside and inside specimen radius, respectively

θ = twist angle in radians

L = specimen height in inches

Figure 18 shows that cumulative shear strain prior to failure was a function of stress ratio, $K/2\sigma_{3c}$, with the greatest change in strain occurring for stress ratios between 0.15 and 0.09. With the exception of Test No. 1, the shear strain based on twist for each test gradually increased with increasing numbers of loading cycles (rotations of principal stresses) until the cycle in

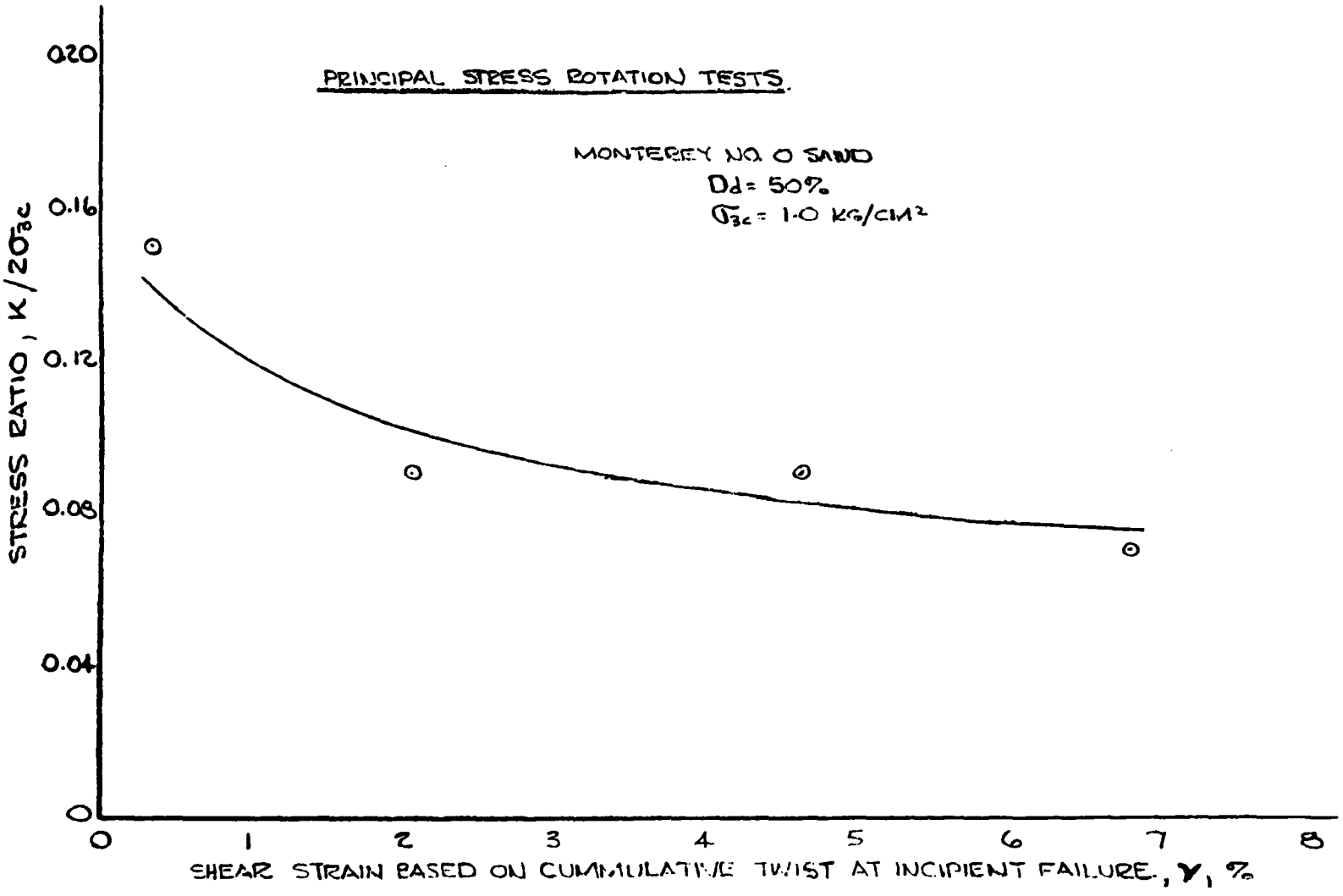

Figure 18. Stress ratio, k/2σ3c , versus shear strain, γ , based on twist at incipient failure

which failure occurred where there was a rapid increase. Twist (and therefore shear strain), however, cycled during each rotation of principal stresses. Greater shear strain occurred during the portion of each cycle when the axial force began placing the specimen in extension and this resulted in the cumulative strain always being in the same direction, i.e., the direction produced by the torque stroke initiated when the maximum axial force was applied in compression. Of the five specimens tested, three failed in extension and two failed in compression. No localized twisting or necking (or bulging in the case of the speciment for Test No. 1) was observed during the portion of the last cycle where failure occurred, thus indicating the specimen preparation procedure produced properties that did not vary significantly from layer to layer.

Strength

33. Since the hollow cylinder specimens were cyclically loaded by rotating the principal planes under a constant deviator stress, failure criteria used for either cyclic simple shear or cyclic triaxial test conditions are not necessarily applicable for these tests. Failure for the hollow cylinder principal stress rotation tests was taken to have occurred when the induced pore pressure equaled the confining pressure and there was no further resistance to deformation, i.e., when liquefaction occurred. In the strength comparisons discussed in the following paragraphs, the number of cycles to 100 percent pore pressure response for the principal stress rotation tests was multiplied by a factor of two since the maximum shear stress was cycled twice in both compression and extension on energy plane during one loading cycle (one complete rotation of the major principal planes).

34. Figure 19 shows a comparison of the strength of Monterey No. 0 sand obtained from the hollow cylinder tests and that obtained from standard cyclic triaxial tests performed by Peacock and Seed (1967) and Mulilis, Chan, and Seed (1975) at the same relative density and confining pressure. Also shown in the figure is a point representing the strength of Monterey No. 0 sand determined from cyclic simple shear tests reported in the investigation by Peacock and Seed (1967). Points representing strengths obtained from cyclic triaxial tests in which specimens were prepared to the same relative density using moist vibration and dry pluviation methods are included in this figure

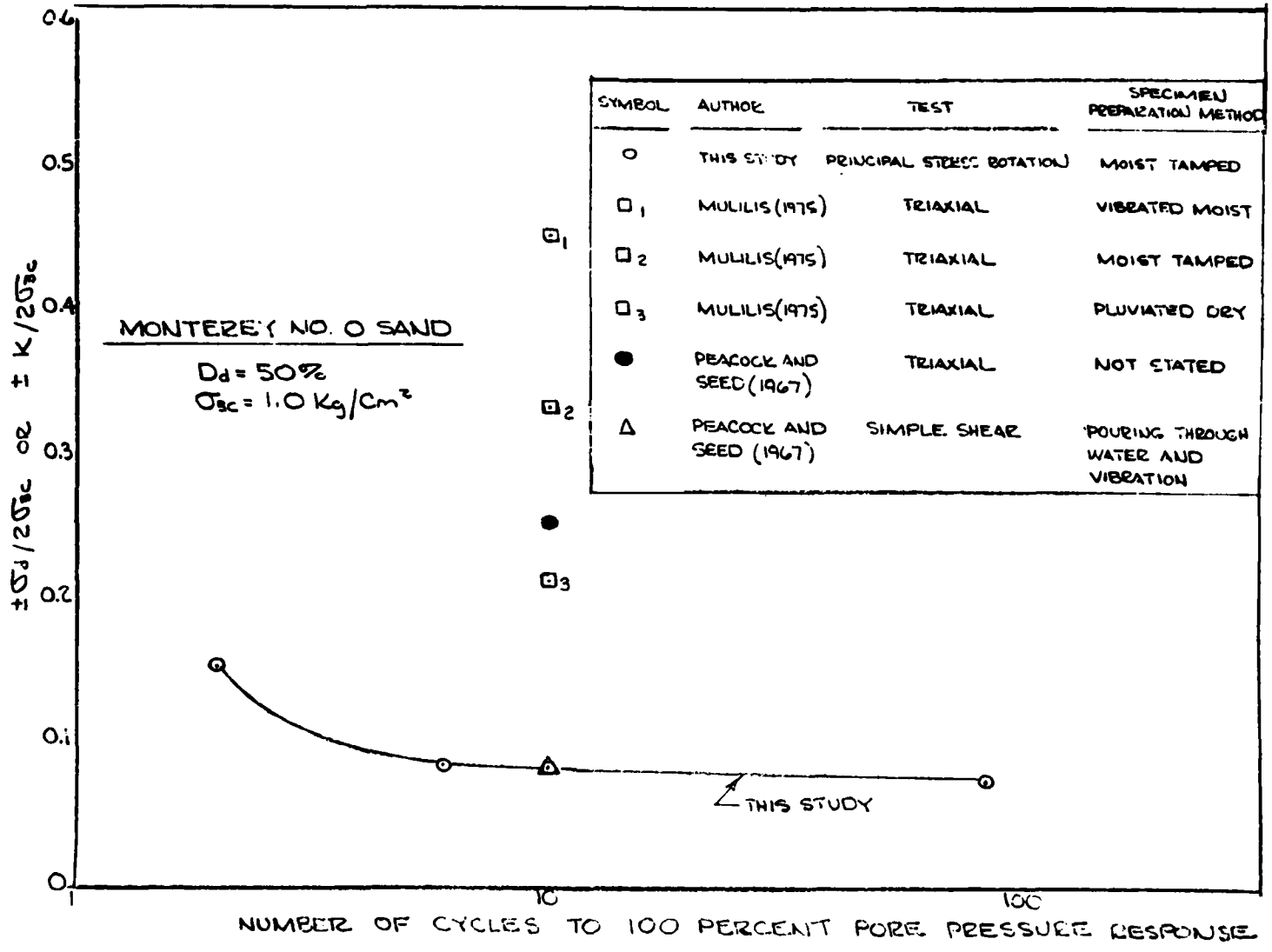

Figure 19. Stress ratio, $\pm\sigma_d/2\sigma_{3c}$ or $\pm k/2\sigma_{3c}$, versus number of cycles to 100 percent pore pressure response

(Fig. 19) to show the wide variation in strength due to varying specimen preparation methods. It should be noted that similar variatons in strength due to the method of specimen preparation may occur for both cyclic simple shear and principal stress rotation tests. It is readily apparent that there is a substantial difference between the strengths determined by cyclic triaxial and hollow cylinder principal stress rotation tests. As may be seen by comparing points based on the same specimen preparation method (moist tamping), the strength based on rotation of principal stresses is only 25 percent of that obtained from cyclic triaxial tests. There is little difference, however, between the stress ratio at 10 cycles shown for the cyclic simple shear test and that for the hollow cylinder test. It is stated in the conclusions of the Peacock and Seed investigation, though, that because of poor specimen placement and uniformity, the stress ratio should be increased by 30 percent. It was also acknowledged that due to poor stress uniformity, the stress ratio should have been increased even more by an unspecified amount.

35. Figure 20 summarizes results of several cyclic shear testing programs utilizing different types of testing apparatus for evaluating liquefaction characteristics. The tests were performed on medium sands at 50 percent relative density with various specimen preparation methods. Theoretically, all of the tests provided stress conditions more similar to in situ conditions than those imposed by cyclic triaxial tests. The seed and Peacock (1971) and Finn, et al. (1971) simple shear and DeAlba, Chan, and Seed (1975) large-scale shake table results most closely approximate the values obtained from the principal stress rotation tests. At lower numbers of cycles, however, complete rotation of major principal planes may be seen to produce liquefaction at substantially lower stress ratios than all of the tests, thus indicating a more severe loading condition during the initial stages of the test. On this basis then, it appears that cyclic principal stress rotation may produce a new lower boundary in laboratory cyclic strength. It should be noted that Wright, Gilbert, and Saada (1978) have attributed the special geometry adopted for the specimens tested by Yoshmi (1973) and Isobashi and Sherif (1974) as providing nonuniform axial normal strains and that the small size of their specimens also impose nonuniform stress conditions due to the small distances between loading boundaries.

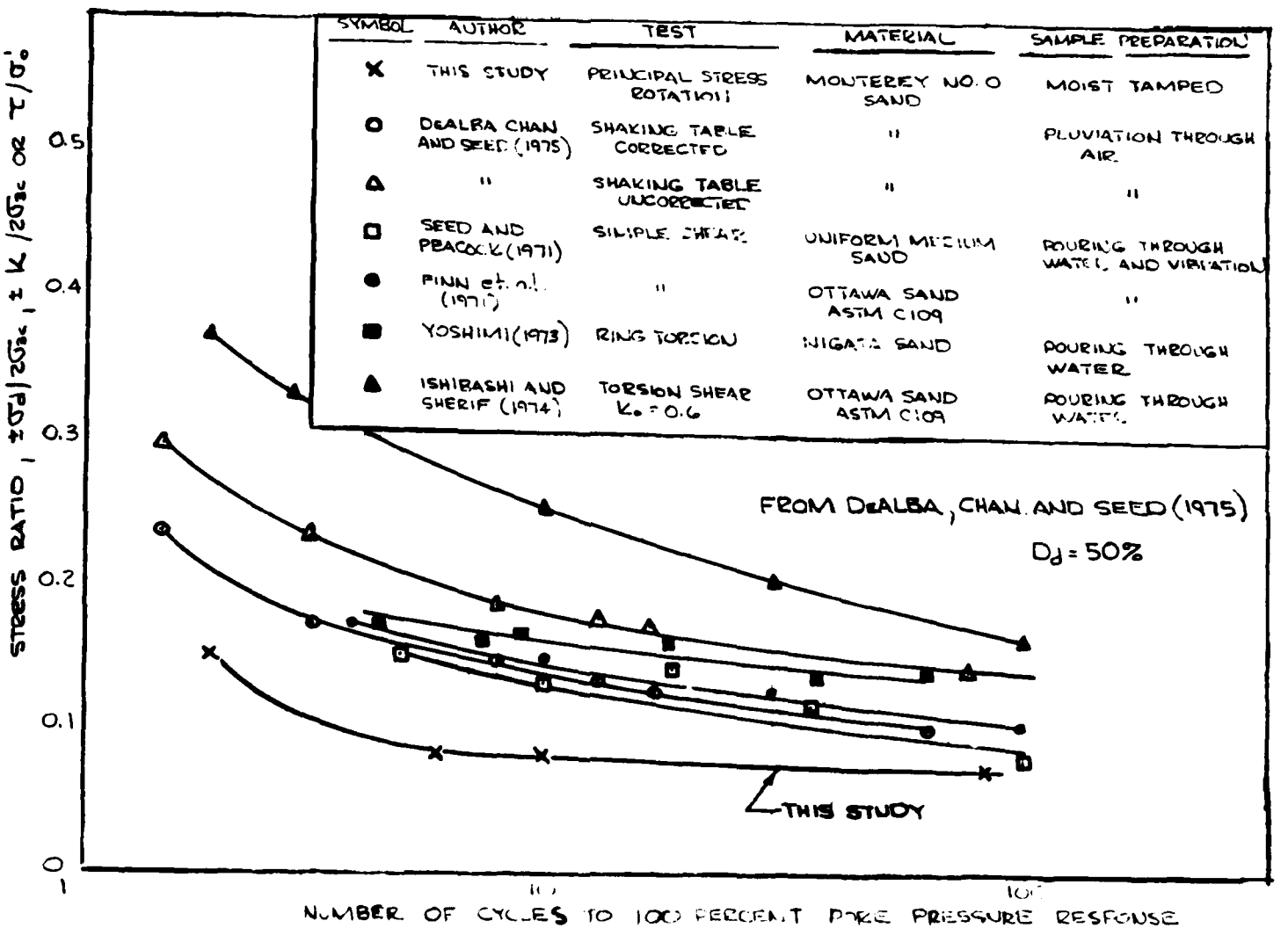

Figure 20. Comparison of principal stress rotation test results with results of other types of cyclic tests

PART VI: CONCLUSIONS AND RECOMMENDATIONS

36. The main objective of this investigation was to investigate the effects of cyclic rotation of principal stresses. To do this it was necessary to first build a testing device that would apply cyclic axial and torsional stresses to a hollow cylinder soil specimen in such a manner that there would be a continuous and systematic rotation of principal stress axes and then to evaluate the performance of the device in a preliminary testing program.

37. The objective was achieved by designing and building a new electropneumatic loading system for an existing hollow cylinder test chamber and by performing five consolidated-undrained hollow cylinder principal stress rotation tests on saturated specimens of Monterey No. 0 sand compacted to 50 percent initial relative density. The confining pressure, σ_{3c}, for each test was 1.0 kg/cm^2.

38. The new apparatus operated in the desired manner and provided some interesting and possibly far-reaching results. The results of the preliminary tests indicate that:

a. Strengths obtained from tests on saturated Monterey No. 0 sand prepared to 50 percent relative density by moist tamping in which principal stresses are rotated are substantially lower than those on the same material determined by either cyclic triaxial or cyclic simple shear tests. Strengths obtained from hollow cylinder principal stress rotation tests may be only one-fourth of those determined by cyclic triaxial tests at high stress ratios.

b. Only slight pore-water pressure variation occurs when the principal stress trajectory is rotated 360 deg in a given cycle. Pore-water pressure, however, steadily increases with increasing numbers of cycles of principal stress rotation until the effective confining pressure is reduced to zero.

c. Prior to failure, specimen deformation due to rotation of the major principal stresses is almost totally in the form of twist. Cumulative rotation of the specimen cap just prior to failure ranged from 0.4 to 17.9 deg and shear strains based on the twist angles ranged from 0.2 to 6.8 percent. Cumulative rotation is always in the direction torque is applied when the specimen is in extension.

d. Principal stress rotation may produce a new lower boundary in laboratory cyclic strength determinations. This is a possibility since all planes in hollow cylinder principal stress rotation test specimens are subjected to the same maximum cyclic shear stress and effects due to anisotropy are included in measured properties.

39. Based on the results of the preliminary testing program, it is recommended that much broader investigations be initiated to:

a. Verify that hollow cylinder principal stress rotation tests provide strengths that represent a lower boundary for cyclic stress tests. The testing program would include cyclic triaxial and simple shear tests on hollow cylinder specimens. Results of these tests would be compared to results obtained from principal stress rotation tests on hollow cylinder specimens prepared using the same method and tested at the same confining pressure.

b. Determine effects of density and confining pressure variation on results of hollow cylinder principal stress rotation tests.

c. Determine effects of different specimen preparation methods on results of hollow cylinder principal stress rotation tests.

d. Examine the complete stress tensor results of two-dimensional earthquake stress wave propagation computer calculations to determine principal stress trajectories calculated as a function of time. Since no way of measuring actual principal stress trajectories due to earthquakes presently exists, this is the only source of insight as to the extent of principal stress trajectory rotation taking place in situ. Some guidance might also be obtained by examining stresses near the surface given by closed form solution for ground motions in homogeneous elastic media due to a point source.

40. It is believed that the development of the WES hollow cylinder principal stress rotation apparatus represents a significant addition to the capability of the U. S. Army Engineer Waterways Experiment Station for investigating the behavior of soils under conditions more closely simulating those actually occurring during earthquake loading and that this capability could lead to designs resulting in safer structures built of and on soils in high earthquake risk areas.

REFERENCES

DeAlba, Pedro, Chan, Clarence K., and Seed, H. Bolton. 1975. "Determination of Soil Liquefaction Characteristics by Large-Scale Laboratory Tests," Report No. EERC 75-14, University of California, Earthquake Engineering Research Center, Berkeley, California.

Finn, W. D. Liam, Pickering, D. J., and Bransby, P. L. 1971. "Sand Liquefaction in Triaxial and Simple Shear Tests," Journal of the Soil Mechanics and Foundation Eivision, American Society of Civil Engineers, Vol 97, No. SM4, April.

Ishibashi, I. and Sherif, M. A. 1974. "Soil Liquefaction by Torsional Simple Shear Device," Journal of the Geotechnical Engineering Division, American Society of Civil Engineers, Vol 100, No. GT8, August.

Mulilis, J. Paul, Chan, Clarence K., and Seed, H. Bolton. 1975. "The Effects of Method of Sample Preparation on the Cyclic Stress-Strain Behavior of Sands," Report No. EERC 75-18, University of California, Earthquake Engineering Research Center, Berkeley, California.

Peacock, W. H. and Seed, H. Bolton. 1967. "Liquefaction of Saturated Sand Under Cyclic Loading Simple Shear Conditions," Report No. TE-67-1, Department of Civil Engineering, University of California, Berkeley, California.

Roscoe, K. H. 1953. "An Apparatus for the Application of Simple Shear to Soil Samples," Proceedings Third International Conference on Soil Mechanics and Foundation Engineering, Vol 1.

Saada, Adel S. 1967. "Stress-Controlled Apparatus for Triaxial Testing," Journal of the Soil Mechanics and Foundations Division, American Society of Civil Engineers, Vol 93, No. SM6, November.

Seed, H. Bolton and Peacock, W. H. 1971. "Test Procedures for Measuring Soil Liquefaction Characteristics," Journal of the Soil Mechanics and Foundations Division, American Society of Civil Engineers, Vol 97, No. SM8, August.

Wright, Daniel K., Gilbert, Paul A., and Saada, Adel S. 1978. "Shear Devices for Determining Dynamic Soil Properties," Proceedings of the ASCE Geotechnical Engineering Division Specialty Conference, Earthquake Engineering and Soil Dynamics, Vol II, Pasadena, California.

Yoshmi, Y. and Ohaka, H. 1973. "A Ring Torsion Apparatus for Simple Shear Tests," Proceedings, Eighth International Conference on Soil Mechanics and Foundation Engineering, Vols 1-2, Moscow.

END

DATE
FILMED

11-83

DTIC